

Half Metallicity in $\text{Pr}_{0.75}\text{Sr}_{0.25}\text{MnO}_3$: A first Principle study.

Monodeep Chakraborty, Prabir Pal, Biju Raja Sekhar

^a*Institute of Physics, Sachivalaya Marg, Bhubaneswar 751 005, India.*

Abstract

In this communication we present a first principle study of $\text{Pr}_{1-x}\text{Sr}_x\text{MnO}_3$ with $x = 0.25$. While the parent compounds of this system are antiferromagnetic insulators with different structural and magnetic ground states, the $x = 0.25$ is in the colossal magnetoresistance regime of the $\text{Pr}_{1-x}\text{Sr}_x\text{MnO}_3$ phase diagram[1]. Our band structure calculations for the end-point compounds matches well with the existing theoretical and experimental results[1,2]. Interestingly, our calculations show that the $\text{Pr}_{0.75}\text{Sr}_{0.25}\text{MnO}_3$ has a half-metallic character with a huge band gap of 2.8 eV in the minority band. We believe this result would fuel further interest in some of these special compositions of colossal magnetoresistive manganites as they could be potential candidates for spintronic devices. We discuss the half-metallicity of the $\text{Pr}_{0.75}\text{Sr}_{0.25}\text{MnO}_3$ in the light of changes in the orbital hybridization as a result of Sr doping in PrMnO_3 . Further, we highlight the importance of half-metallicity for a consolidated understanding of colossal magnetoresistance effect.

Key words: A. Colossal magnetoresistance; C. Half-Metallicity; D. Electronic structure

PACS: 75.47.Gk; 72.25.-b; 71.20.-b

1 Introduction

The colossal magnetoresistance (CMR) materials have attracted a lot of attention of the condensed matter community owing to their spectacular insulator-metal transition with magnetic field. Ferromagnetic $\text{A}_{1-x}\text{B}_x\text{MnO}_3$ (A = rare earth, B = alkaline earth) exhibits CMR properties at particular concentrations of x in their respective phase diagrams. Half-Metallicity (HM) has been observed in a few of these compounds both theoretically and experimentally[3,4]. In case of half-metals one of the spin bands (generally the majority

Email address: monodeep@iopb.res.in; Tel:+91-674-2301058; Fax:+91-674-2300142 (Monodeep Chakraborty).

band) is conducting whereas the other band (generally the minority band) is insulating at the Fermi level (E_F). This facilitates 100% spin polarization. This property of the half-metals make them potential candidates for application in spintronic devices and magnetic sensors. The CMR effect along with high spin polarization add to the technological importance of the CMR manganites. Apart from their great potential in technology, the strong interplay of the spin, orbital and charge degrees of freedom of the charge carriers involved in this insulator-metal transition, holds out a promise for rich physics.

In this paper we have done a first principle Tight Binding- Linearized Muffin Tin Orbital (TB-LMTO)[5,6] calculation of the end-point compositions of $\text{Pr}_{1-x}\text{Sr}_x\text{MnO}_3$ and with $x = 0.25$ doping. For SrMnO_3 we have done the calculation with local spin density approximation (LSDA). For PrMnO_3 and $\text{Pr}_{0.75}\text{Sr}_{0.25}\text{MnO}_3$ we had to incorporate the electron-electron correlation (LSDA+U) to account for the band gap in PrMnO_3 and to match our results with the available spectroscopic data. Moreover, the charge and orbital order observed in doped manganites also merits a LSDA+U treatment in order to account for the intra-shell (d and f) Coulomb interaction[7]. All the three calculations have been done with Vosko-Ceperley-Alder parametrization for the exchange correlation energy and potential. We have included Langreth-Mehl-Hu gradient corrections to the exchange correlation. The k-mesh used for all these self-consistent calculations was $10 \times 10 \times 10$. Although, SrMnO_3 can take both cubic as well as hexagonal structures[2], here we have considered only the cubic (distorted) polymorph of this perovskite since our main motivation is to study the HM in $\text{Pr}_{0.75}\text{Sr}_{0.25}\text{MnO}_3$. We have also compared the band structure results of $\text{Pr}_{0.75}\text{Sr}_{0.25}\text{MnO}_3$ with the end-point compounds. Crystal structure of the PrMnO_3 system is taken from a published neutron diffraction data. For $\text{Pr}_{0.75}\text{Sr}_{0.25}\text{MnO}_3$ we have taken the same structure as PrMnO_3 with one Pr atom replaced by a di-valent Sr.

Electron-lattice coupling (ELC) has a very important role in the physics of manganites. They show up in two ways. First is the so called "tolerance factor"[8] involving the static effect of crystal structure on electron hopping, which has a direct effect on conductivity. The atomic size difference between the rare-earth atoms and the divalent dopants results in an internal stress which effects the Mn-O-Mn bonds. The electron hopping between the Mn sites is inversely proportional to the compression of the Mn-O-Mn bonds. This type of ELC of PrMnO_3 has been taken in to account in our calculations. The importance of different Jahn-Teller modes and polarons in accounting the proper insulating A-type antiferromagnetic (AFM) ground state of undoped LaMnO_3 has been dealt by several groups[3,9,10]. The second type of ELC is the dynamic ELC which couples the lattice vibration (phonons) with electronic degrees of freedom. Since TB-LMTO calculations are based on adiabatic approximation which decouples the electronic and the lattice degrees of freedom[8], accounting for the dynamic ELC is beyond the scope of this work.

Band structure calculations can provide only a qualitative description of any system as the structural complications that exist in real systems are difficult to accommodate in a calculation. Although, we assume proper stoichiometry, cation vacancy and oxygen-non stoichiometry are a common in real systems. Again in $\text{Pr}_{0.75}\text{Sr}_{0.25}\text{MnO}_3$ we have assumed the crystal structure of PrMnO_3 . The effect of Pr/Sr disorder and local strains and relaxations have not been taken into account. But still our prediction of HM in

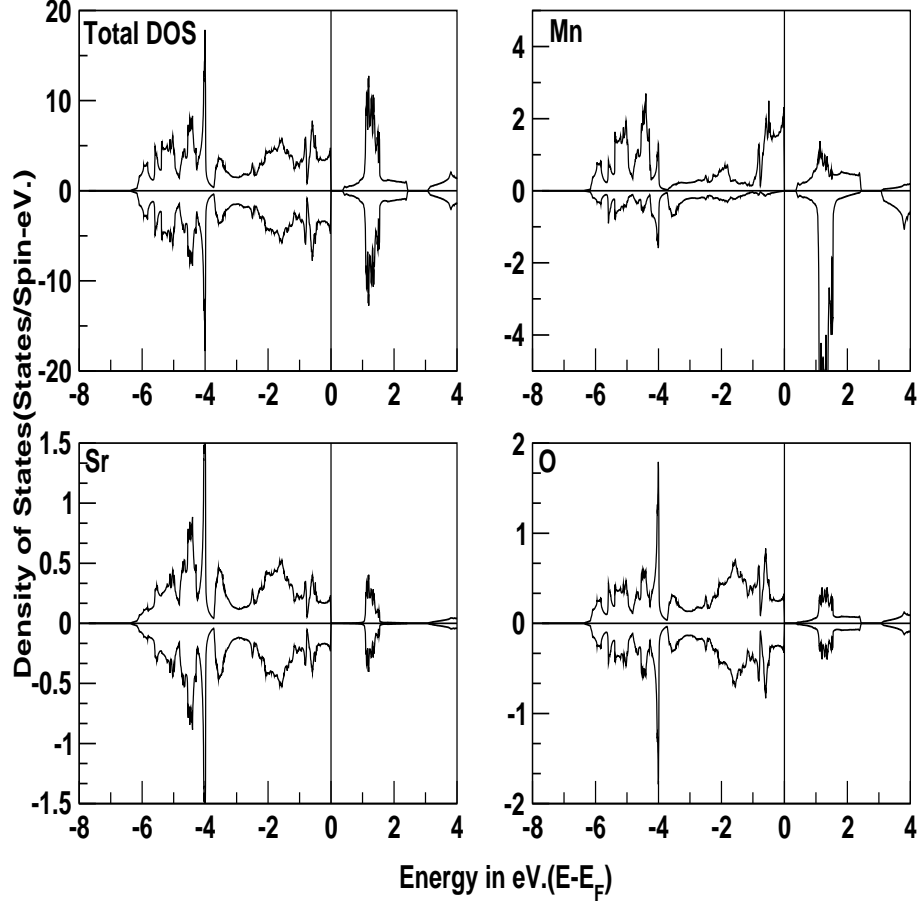


Fig. 1. The spin resolved total and site projected density of states of SrMnO_3 . The top left panel depicts the total density of states for the majority and minority band. The band gap is 0.34 eV. The top right panel shows the spin resolved Mn PDOS. The bottom left panel shows the Sr PDOS and the bottom right shows the O PDOS.

$\text{Pr}_{0.75}\text{Sr}_{0.25}\text{MnO}_3$ is robust enough to merit attention.

2 SrMnO_3

Cubic SrMnO_3 has a G-type AFM ground state with a lattice parameter[2] of 3.824 Å. Our calculations with different magnetic configurations have shown that this G-type AFM state turns out to be the most stable, in agreement with earlier reports[2]. In this work we have used only the G-type AFM structure. Results of our TB-LMTO (LSDA) calculations are shown in fig.1. The total and site projected density of states (PDOS) clearly reveals a band gap of 0.34 eV which is similar to that obtained by other band structure calculations[2] on this system. The near E_F states are dominated by Mn 3d and O 2p. The near E_F valence band shows a strong Mn 3d - O 2p hybridization. Although, Sr states have a very little presence near E_F , they appear to be hybridized with the significant O states throughout the valence band. It is clear from the figure that the conduction states are dominated mainly by Mn. We have estimated the magnetic moment of individual

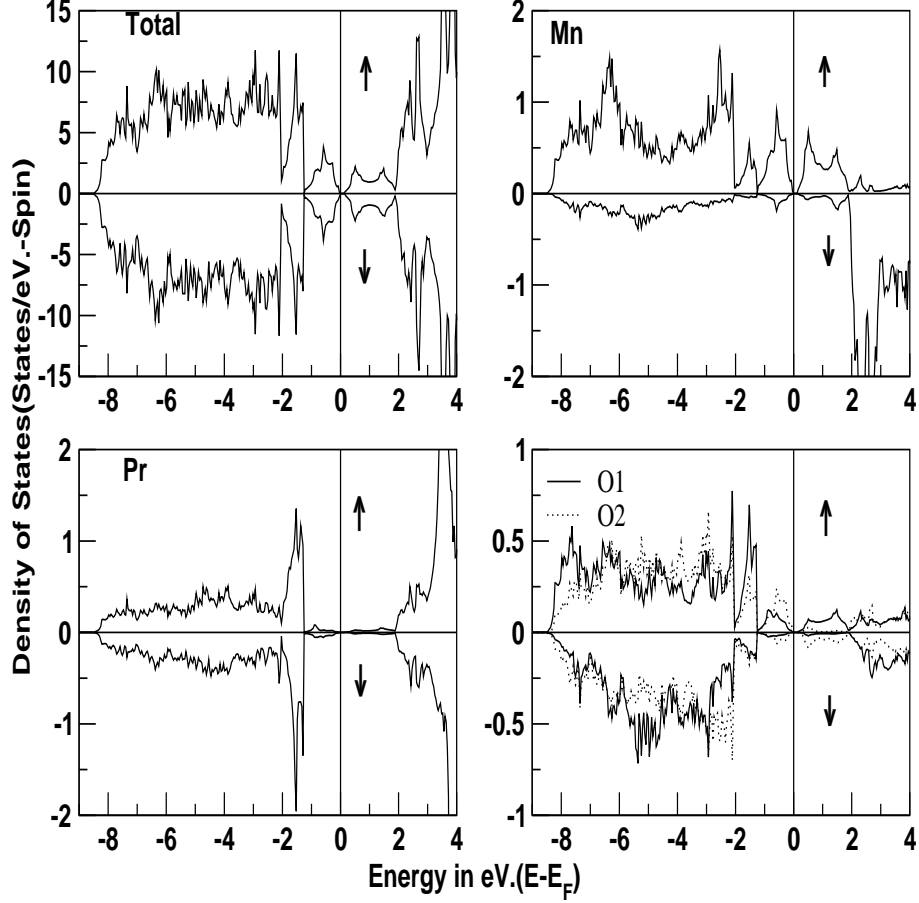


Fig. 2. The spin resolved total and site projected density of states of PrMnO_3 . The top left panel depicts the total density of states for the majority and minority band. The band gap is 0.11 eV. The top right panel shows the spin resolved Mn PDOS. The bottom left panel shows the Pr PDOS and the bottom right shows the O1/O2 PDOS.

Mn atom to be $2.48 \mu_B$ which is again similar to $2.47 \mu_B$ obtained by calculations using the Vienna Ab-Initio Simulation Package (VASP)[2]. This value of the magnetic moment, which is lower compared to that of free Mn^{4+} ion ($3 \mu_B$, neglecting the orbital contribution), indicate the strong hybridization of the Mn and O states in cubic SrMnO_3 . It should be noted that the shape of the O PDOS and the Mn PDOS near E_F have striking similarities, which hints to a strong covalent bonding. This inference is supported by the Crystal orbital Hamiltonian population (COPH) analysis done by Rune Sondena et al. [2].

3 PrMnO_3

LSDA+U band-structure calculations for PrMnO_3 were done for the A-type AFM phase using the crystal structure (space group: $\text{Pbnm}(62)$) taken from a neutron diffraction result[11] published earlier. The LSDA+U method was employed mainly to account for the strong electron correlation which is behind the insulating nature of this material[1].

Unlike in LaMnO_3 where simple LSDA can reproduce the band gap, in PrMnO_3 the LSDA+U treatment is essential to derive a realistic value of the gap. In our calculation, we have taken the exchange term J and the correlation term U for Pr $4f$ state to be 0.95 eV and 7 eV respectively and those for Mn $3d$ to be 0.87 eV and 4 eV respectively.

Fig. 2 shows the spin resolved total and site projected density of states of PrMnO_3 . Our LSDA+U calculation shows an insulating A-type AFM ground state for PrMnO_3 . We have estimated the band gap to be 0.11 eV. Here, the electron-electron correlation that has been incorporated, was found to be crucially important for obtaining the band gap. A simple LSDA calculation of this system does not give an insulating ground state. Further, the LSDA calculation results in the Pr $4f$ states appearing very close to the E_F , contrary to the photoemission spectroscopic results showing these states to be 2 eV below the E_F . LSDA+U calculation enables us to fix this problem to certain extent. The Pr states have hardly any presence near E_F . The near E_F PDOS of Mn and O1/O2 makes an interesting study. Though, the Mn and O1/O2 states are hybridized near E_F , here this hybridization is not as strong as in the cubic SrMnO_3 . Moreover, in this system, the hybridization between Mn and O2 is certainly stronger than that between Mn and O1, owing to greater physical proximity of Mn with O2 than O1. Here, the degree of covalency of Mn-O2 bond is certainly less than that we saw in cubic SrMnO_3 .

Another interesting observation is that, the hybridization of Mn $3d$ and the O1/O2 ($2p$) states are clearly spin dependent. While there is a considerable hybridization in the majority band, both types of oxygen atoms hardly have any significant weight in the minority band indicting a strong spin dependence to the Mn-O1/O2 hybridization. Here the magnetic moment of individual Mn atom in PrMnO_3 is $3.94 \mu_B$ which is comparable to the magnetic moment of free Mn^{3+} , neglecting the orbital contribution. This suggests a strong atomic like moment of Mn in PrMnO_3 and a relatively weak hybridization compared to that in SrMnO_3 . The magnetic moment of O1 atom is $\approx 0.035 \mu_B$ and that of O2 atom is $\approx 0.05 \mu_B$. The relatively higher magnetic moment of O2 atom could be due to its proximity with the Mn atom.

4 $\text{Pr}_{0.75}\text{Sr}_{0.25}\text{MnO}_3$ and Half-Metallicity

The band-structure calculation (LSDA+U) on $\text{Pr}_{0.75}\text{Sr}_{0.25}\text{MnO}_3$ were done for the ferromagnetic phase. The crystal structure that we have used for $\text{Pr}_{0.75}\text{Sr}_{0.25}\text{MnO}_3$ super-cell calculation is that of the parent compound PrMnO_3 . We have substituted one of the Pr atoms with a Sr atom in the four formula unit cell. The exchange term J and the correlation term U for Pr $4f$ and Mn $3d$ are the same as those used for PrMnO_3 . In fig. 3 we present the calculated total and site projected density of states of $\text{Pr}_{0.75}\text{Sr}_{0.25}\text{MnO}_3$. We have chosen this composition in order to study the ferromagnetic metallic ground state of $\text{Pr}_{1-x}\text{Sr}_x\text{MnO}_3$ at this doping. Also, this particular composition is easy to handle in the LSDA+U. A comparison of our results with the results from photoemission experiments on a close composition in ferromagnetic metallic phase can be found elsewhere[12]. There is a qualitative matching between our band structure results and the spectroscopic data. The most prominent effect of substituting one of the Pr with Sr is the appearance of a

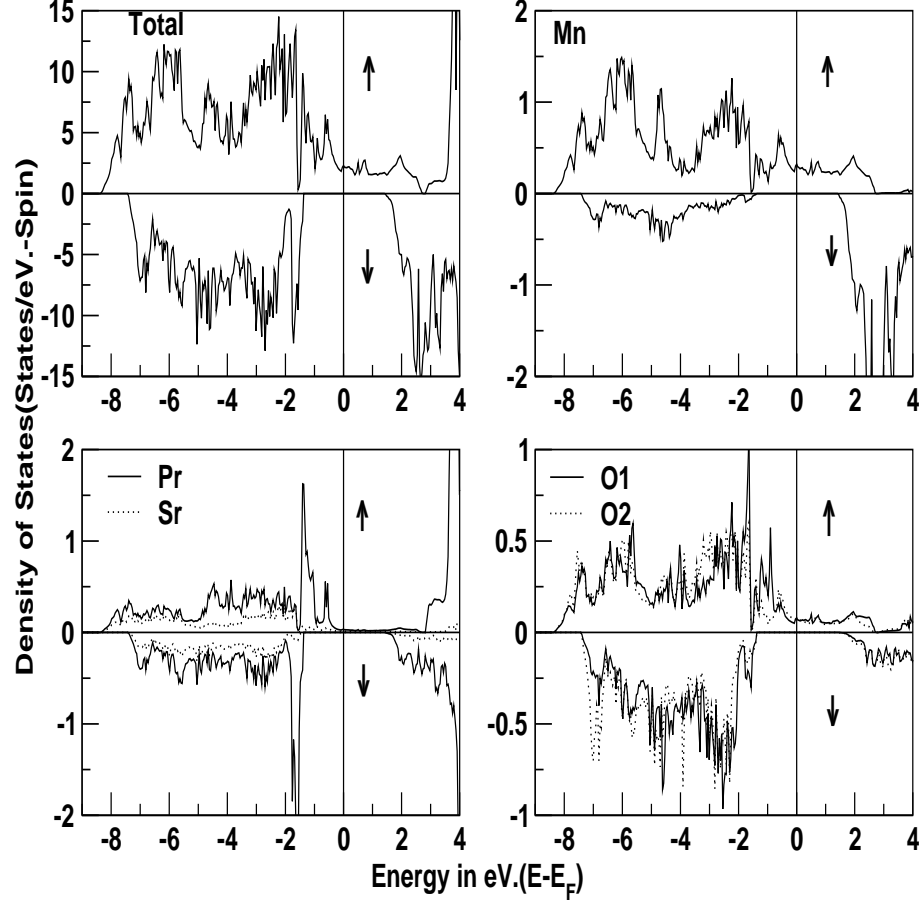


Fig. 3. The spin resolved total and site projected density of states of $\text{Pr}_{0.75}\text{Sr}_{0.25}\text{MnO}_3$. The top left panel depicts the total density of states for the majority and minority band. The minority band gap is 2.8 eV. The top right panel shows the spin resolved Mn PDOS. The bottom left panel shows the Pr/Sr PDOS and the bottom right shows the O1/O2 PDOS.

finite DOS at E_F in the majority band of the total spin polarized DOS, while the minority band display a wide gap insulating behavior. The band gap in the minority band is 2.8 eV. Appearance of this metallicity upon 25% Sr doping is consistent with the phase diagram reported earlier[1]. We will discuss the half-metallicity upon Sr doping by comparing these results with those from the end-point compounds, especially with PrMnO_3 .

Since our focus is on HM, we will concentrate on the states near E_F . The Pr/Sr states have hardly any role near E_F . The Sr PDOS in SrMnO_3 , though not significant, has a larger band width in the valence band compared to that found in $\text{Pr}_{0.75}\text{Sr}_{0.25}\text{MnO}_3$. This could be because of the Sr acting more like an impurity atom. Pr PDOS in the majority band shows a certain degree of hybridization with the O1 atom near 1 eV below the E_F . The near E_F states here also are dominated by the Mn and O. From the Mn and O PDOS, it is quite clear that there is a strong hybridization between the Mn 3d and the O 2p states which is spin dependent. Here both the O1 and O2 hybridization with the Mn are stronger than the undoped PrMnO_3 in the majority band. The O1 2p shows the same degree of hybridization at E_F as that of O2 2p states, which was not the case in PrMnO_3 . We attribute this significant change to Sr doping. Comparing the

shape of O1 and O2 with those of the Mn sites in the majority band, we conjecture that Sr doping in PrMnO_3 increases the degree of covalency between the Mn 3d and O1/O2 2p states. Consequently, the gap in the majority band is filled up and gives rise to metallicity. Whereas, in the minority band both the Mn and O1/O2 states are pushed further apart from the E_F giving rise to a band gap of 2.8 eV. The calculated magnetic moment of individual Mn atom in $\text{Pr}_{0.75}\text{Sr}_{0.25}\text{MnO}_3$ is $3.88 \mu_B$, which is less than that of Mn atom in PrMnO_3 , again suggesting an increased hybridization activity. Simultaneously, the magnetic moment of O1 and O2 in $\text{Pr}_{0.75}\text{Sr}_{0.25}\text{MnO}_3$ also increases slightly (by $\approx 0.01 \mu_B$) validating our conjecture of increased hybridization activity upon Sr doping. The individual Mn atoms of $\text{Pr}_{0.75}\text{Sr}_{0.25}\text{MnO}_3$ lose approximately 0.05e charge compared to the Mn atoms of PrMnO_3 . This is due to the majority e_g electrons which fill up the band gap in the majority band as a result of the hybridization of Mn with O states. The total magnetic moment of the Super Cell is $15 \mu_B$. The integral magnetic moment is the signature of the resulting HM. The magnetic moment of Mn_{Pr-Pr} atom is $3.886 \mu_B$ and that of Mn_{Pr-Sr} is $3.878 \mu_B$. The difference in charge between the two types of Mn are 0.002e. This shows that the difference in charge and magnetic moment between the two inequivalent Mn atoms are insignificant. There is hardly any difference between the two types of Mn sites in their spin projected PDOS, with both types of Mn atoms contributing to the near E_F minority band. Pickett et. al. [3] have tried to explain the HM as an effect of the A/B local environment disorder, creating a variation in the Mn d site energy which in turn induces localization effects in the near E_F minority band making it non-conducting. This does not seem to be the case from our study. We think the spin-dependent hybridization of Mn 3d and O 2p which was present in the PrMnO_3 is further strengthened upon hole (Sr) doping and this is responsible for HM in $\text{Pr}_{0.75}\text{Sr}_{0.25}\text{MnO}_3$.

The HM character also can account for the high resistivity at zero field. Since only single spin band can participate in the conductivity process, electron hopping between ferromagnetic regions with opposite directions of magnetization become negligible leading to high resistivity. Here, the scattering process will not randomize the direction of propagation of the electron as would have been the case for random potential (spin) arrangement. Here the electron would suffer a barrier reflection due to the ferromagnetic regions of opposite magnetization. This effect is further accentuated in case of HM (compared to other systems like magnetic multilayers), as there is no minority conduction. When a magnetic field is applied forcing the different ferromagnetic regions to align along the magnetic field, there appears a sharp drop in resistivity. This strong insulating behaviour at zero field and subsequent melting of different ferromagnetic regions on application of magnetic field could contribute substantially to the large negative magnetoresistance.

5 Conclusions

We have studied the $\text{Pr}_{1-x}\text{Sr}_x\text{MnO}_3$ with $x = 0.25$ using a first principle band structure calculation method of LSDA+U. Our calculations show that the CMR system $\text{Pr}_{0.75}\text{Sr}_{0.25}\text{MnO}_3$ has a half-metallic character with a band gap of 2.8 eV in the minority band. We have compared the band structure of this compound with that of its parent compositions. Also,

our results for the parent compounds match well with the existing theoretical and experimental results. We have discussed the half-metallicity of $\text{Pr}_{0.75}\text{Sr}_{0.25}\text{MnO}_3$ in the light of changes in spin-dependent hybridization of Mn $3d$ and O $2p$ upon hole doping. We have also highlighted the importance of half-metallicity for a consolidated understanding of CMR effect.

One of the authors (M.C) would like to acknowledge the helpful discussions with Eva Pavarini (Forschungszentrum Juelich) and Manuel Richter (IFW Dresden).

References

- [1] C. Martin, A. Maignan, M. Hervieu, B. Raveau, Phys. Rev. B 60 (1999) 12191.
- [2] Rune Sondena, P. Ravindran, Svein Stolen, Tor Grande, Michael Hanfland, Phys. Rev. B 74 (2006) 144102.
- [3] W. E. Pickett, D. J. Singh, Phys. Rev. B 53 (1996) 1146.
- [4] J.-H. Park, E. Vescovo, H.-J. Kim, C. Kwon, R. Ramesh, T. Venkatesan, Nature 392 (1998) 794.
- [5] V. I. Anisimov, J. Zaanen, O. K. Andersen, Phys. Rev. B 44 (1991) 943.
- [6] V. I. Anisimov, F. Aryasetiawan, A. I. Lichtenstein, J. Phys. Condens. Matter 9 (1997) 767.
- [7] V. I. Anisimov, I. S. Elfimov, M. A. Korotin, K. Terakura, Phys. Rev. B 55 (1997) 15494.
- [8] A. J. Millis, Nature 392 (1998) 147.
- [9] S. Satpathy, Z. S. Popovic and F. R. Vukajlovic Phys. Rev. Lett. 76 (1996) 960.
- [10] N. Hamada, H. Sawada, and K. Terakura, in Spectroscopy of Mott Insulators and Correlated Metals, edited by A. Fujimori and Y. Tokura, Springer-Verlag, Berlin, (1995) pp. 95-105.
- [11] Z. Jirak, S. Krupicka, Z. Simsa, M. Dlouha, S. Vartislav, J. Magn. Magn. Mater. 53 (1985) 153.
- [12] P. Pal, M. K. Dalai, R. Kundu, M. Chakraborty, B. R. Sekhar, C. Matin, Phys. Rev. B 76 (2007) 195120.